ANTICANCER RESEARCH *42*: 589-598 (2022)
doi:10.21873/anticanres.15516

Suppression of DYRK1A/B Drives Endoplasmic Reticulum Stress-mediated Autophagic Cell Death Through Metabolic Reprogramming in Colorectal Cancer Cells

JIEON HWANG[1,2*], AREUM PARK[3,4*], CHINWOO KIM[1,2], DANBI YU[1,2], HYUNGJU BYUN[1,2], MINHEE KU[5,6], JAEMOON YANG[5,6], TAE IL KIM[7], KYU-SUNG JEONG[4], KI YOUNG KIM[3,8], HYUK LEE[3,9] and SANG JOON SHIN[2,10]

[1]Department of Medicine, Yonsei University College of Medicine, Seoul, Republic of Korea;
[2]Songdang Institute for Cancer Research, Yonsei University College of Medicine, Seoul, Republic of Korea;
[3]Infectious Diseases Therapeutic Research Center, Korea Research Institute of Chemical Technology, Daejeon, Republic of Korea;
[4]Department of Chemistry, Yonsei University, Seoul, Republic of Korea;
[5]Department of Radiology, Yonsei University College of Medicine, Seoul, Republic of Korea;
[6]Severance Biomedical Science Institute, Yonsei University College of Medicine, Seoul, Republic of Korea;
[7]Division of Gastroenterology, Department of Internal Medicine, Yonsei University College of Medicine, Seoul, Republic of Korea;
[8]Drug Discovery Platform Technology Research Center, Korea Research Institute of Chemical Technology, Daejeon, Republic of Korea;
[9]Graduate School of New Drug Discovery and Development, Chungnam National University, Daejeon, Republic of Korea;
[10]Division of Medical Oncology, Department of Internal Medicine, Yonsei Cancer Center, Yonsei University College of Medicine, Seoul, Republic of Korea

Abstract. *Background/Aim: We previously identified KS40008 (4-(3-(4-hydroxyphenyl)-1H-pyrazolo[3,4-b]pyridin-5-yl)benzene-1,2-diol), a novel inhibitor of dual-specificity tyrosine phosphorylation-regulated kinase family (DYRK) 1A/B, which exhibited high enzymatic activity and cell proliferation-inhibitory effects in colorectal cancer (CRC) cell lines. In the present study, we aimed to elucidate the antitumor mechanisms of KS40008. Materials and Methods: To assess the cytotoxicity of KS40008, we utilized a human cell line and organoid model and performed a CCK-8 assay and real-time cell analysis. Mitochondrial function was determined through mitochondrial staining, mito-stress test, and glycolysis test. In addition, we investigated the mechanisms of cancer cell death induced by KS40008 through immunoblotting, real-time quantitative polymerase chain reaction, reactive oxygen species staining, and immunofluorescence staining. Results: KS40008 exhibited significant cytotoxicity in CRC and non-CRC cell lines, and organoid models compared to 5-fluorouracil, a conventional chemotherapeutic drug. Moreover, KS40008-induced inhibition of DYRK1A/B led to mitochondrial dysfunction and endoplasmic reticulum stress, promoting autophagic cancer cell death. Conclusion: KS40008 exerts antitumor activity through the inhibition of DYRK1A/B. Here, we demonstrated a mechanism by which KS40008 affects endoplasmic reticulum stress-mediated autophagy through the induction of mitochondrial stress, leading to cytotoxicity in CRC.*

Cancer cells have developed multiple pathways to regulate cellular responses to conditions such as endoplasmic reticulum (ER) stress, hypoxia, and deprivation of nutrients (1). The ER is the organelle responsible for protein synthesis

*These Authors contributed equally to this study.

Correspondence to: Hyuk Lee, Ph.D., Infectious Diseases Therapeutic Research Center, Korea Research Institute of Chemical Technology, 114, Gajeong-ro, Daejeon, Republic of Korea. Tel: +82 1077218211, Fax: +82 428607160, e-mail: leeh@krict.re.kr and Sang Joon Shin, MD, Ph.D., Division of Medical Oncology, Department of Internal Medicine, Yonsei Cancer Center, Yonsei University College of Medicine, 50-1 Yonsei-ro, Seoul, Republic of Korea. Tel: +82 222288138, Fax: +82 222278073, e-mail: ssj338@yuhs.ac

Key Words: DYRK1A protein, DYRK1B protein, protein kinases, endoplasmic reticulum stress, autophagy, colorectal cancer.

in eukaryotic organisms. Subsequently, the accumulation of unfolded or misfolded proteins causes the unfolded protein response, which leads to sustained ER stress (2, 3). Key sensors are activated due to ER stress, including protein kinase R-like endoplasmic reticulum kinase, general control nonderepressible 2, and eukaryotic translation initiation factor-2α (EIF2A) (4-6). Phosphorylation of EIF2A further triggers activating transcription factor 4 (ATF4), which in turn stimulates expression of C/EBP homologous protein (CHOP) (7). ATF4 is a key regulator that mediates the transcription of genes involved in antioxidant response, autophagy, amino acid transport, and protein synthesis (8, 9). While regulation of ER stress can maintain the survival of cancer cells, excessive ER stress has been implicated in several human pathophysiologies, including cancer (7) but can also trigger autophagy, leading to cancer cell death (10). Therefore, ER stress is important in determining cell fate.

The dual-specificity tyrosine phosphorylation-regulated kinase family (DYRK) comprises DYRK1A, DYRK1B, DYRK2, DYRK3, and DYRK4 (11). DYRKs phosphorylate substrates involved in cellular processes such as proliferation and cell cycle regulation (12, 13) and have been associated with cancer cell survival and differentiation (12). Among them, DYRK1A and DYRK1B are particularly expressed in a tumor-specific pattern, suggesting poor prognosis and are potential attractive biomarkers (12, 14). Inhibition of DYRK1A and DYRK1B can specifically suppress cancer cell growth, however, the mechanisms of DYRK1A and DYRK1B action in colorectal cancer (CRC) cells are poorly understood. Recently, we reported that a novel DYRK1A/B inhibitor, 4-(3-(4-hydroxyphenyl)-1*H*-pyrazolo[3,4-*b*]pyridine-5-yl)benzene-1,2-diol (KS40008) (Figure 1A) (previously referred to as Comp 8h) was identified through the suppression of DYRK1A and -1B enzymatic activity with half-maximal inhibitory concentration (IC_{50}) values of 5 nM and 3 nM, respectively (15).

In the present study, we aimed to elucidate the molecular mechanisms of KS40008 as a novel DYRK1A/B inhibitor in CRC cells. Our findings revealed that KS40008-induced DYRK1A/B inhibition led to autophagic cell death through the activation of the ER stress response, suggesting that KS40008 might be utilized to contribute to chemotherapy of CRC.

Materials and Methods

Cell culture. Eleven CRC cell lines (COLO205, DLD-1, HCT116, HCT15, HT29, LS1034, LS174T, RKO, SW480, and SW620) and nine non-CRC cell lines (A549, DU145, HeLa, Huh7, MCF7, MDAMB231, PANC-1, PC3 and SKNMC) were obtained from the Korean Cell Line Bank (Seoul, Republic of Korea) and maintained in Dulbecco's modified Eagle's medium or Roswell Park Memorial Institute 1640 (Lonza, Basel, Switzerland) containing 10% fetal bovine serum, 100 U/ml penicillin, and 100 μg/ml streptomycin under 5% CO_2 at 37˚C.

Cell viability assay. CRC and non-CRC cell lines were dispensed into 96-well plates at a density of 2×10^4 cells/well and allowed to attach for 24 h. Cells were treated with KS40008 at concentrations of 0.0001 to 100 μM for 48 h. Cells were then incubated in 10 μl of CCK-8 (Dojindo, Kumamoto, Japan) for 3 h at 37˚C. The absorbance was subsequently measured at 450 nm using a microplate reader (Molecular Devices, San Jose, CA, USA). IC_{50} values were calculated using GraphPad Prism 5 (GraphPad Software, San Diego, CA, USA).

Organoid viability assay. Human CRC organoids were provided by the laboratory of Tae Il Kim. Organoids were maintained with the following vital components: 1x glutamax (Gibco, Carlsbad, CA, USA), 1x N2 supplement (Gibco), 1x B27 supplement (Gibco), 1 mM *N*-acetyl-L-cysteine (Sigma, St Louis, MO, USA), 2 mM L-glutamine (Sigma), 10 mM nicotinamide (Sigma), 500 nM A83-01 (Sigma), 10 μM SB202190 (Sigma), 10 nM gastrin I (Sigma), and 50 ng/ml human epidermal growth factor (Peprotech, East Windsor, NJ, USA). The CRC organoids were passaged every 1-2 weeks using mechanical dissociation.

To assess viability, CRC organoids were treated with KS40008 or 5-fluorouracil (5-FU) at concentrations ranging from 0.1 to 100 μM for 5 days and then incubated with CellTiter-Glo 3D cell viability reagent (Promega, Madison, WA, USA) according to the manufacturer's instructions. Luminescence was measured using a microplate reader (Molecular Devices) and images were obtained using Operetta CLS (PerkinElmer, Waltham, MA, USA). IC_{50} values were estimated using GraphPad Prism 5 (GraphPad Software, San Diego, CA, USA).

Real-time cell analysis. The cell growth rate and inhibitory effect of KS40008 treatment were monitored using a real-time cell analysis system. Gold microelectrodes covering the bottom surface of each well of an E-plate enabled a readout of impedance in the electron flow caused by the adherence of cells. The cell index (CI) parameter derived from impedance data is dependent on the number, size, and shape of the cell and its cell-substrate attachment quality. CI values are calculated as shown in the following equation (16):

$$CI=Z-Z15\zeta\ [i=1, 2, 3, 4, \ldots, N]$$

In which Z_i is the impedance at an individual point of time during the experiment; Z_0 is the impedance at the start of the experiment; *i* is 1, 2, 3, …, *N*; *N* is the time point of measurements (16, 17). The CI was normalized by dividing the CI value at different time points after KS40008 administration by the baseline CI value.

The E-plates (ACEA Biosciences, San Diego, CA, USA) were engaged with the xCeLLigence™ DP system (Roche Diagnostics GmbH, Penzberg, Germany) after the addition of growth medium (100 μl) to plot the baseline value. The background impedance was recorded in each well, followed by seeding of 5×10^4 cells. The cells were incubated for 15 min at room temperature until fully settled and re-engaged onto the device. After 24 h, each well was treated with KS40008 (1 or 5 μM) and continuously monitored at 30-min intervals during the experiment.

Cell energy phenotype test. Cellular energy phenotypes and metabolic switches were measured using a Seahorse XFe24 Analyzer (Agilent Technologies, Inc., Santa Clara, CA, USA). After the initial measurements, HCT116 and SW480 cell cultures were exposed to 5 or 10 μM KS40008 for 24 h the following day. The cells were seeded in growth medium at an optimized density

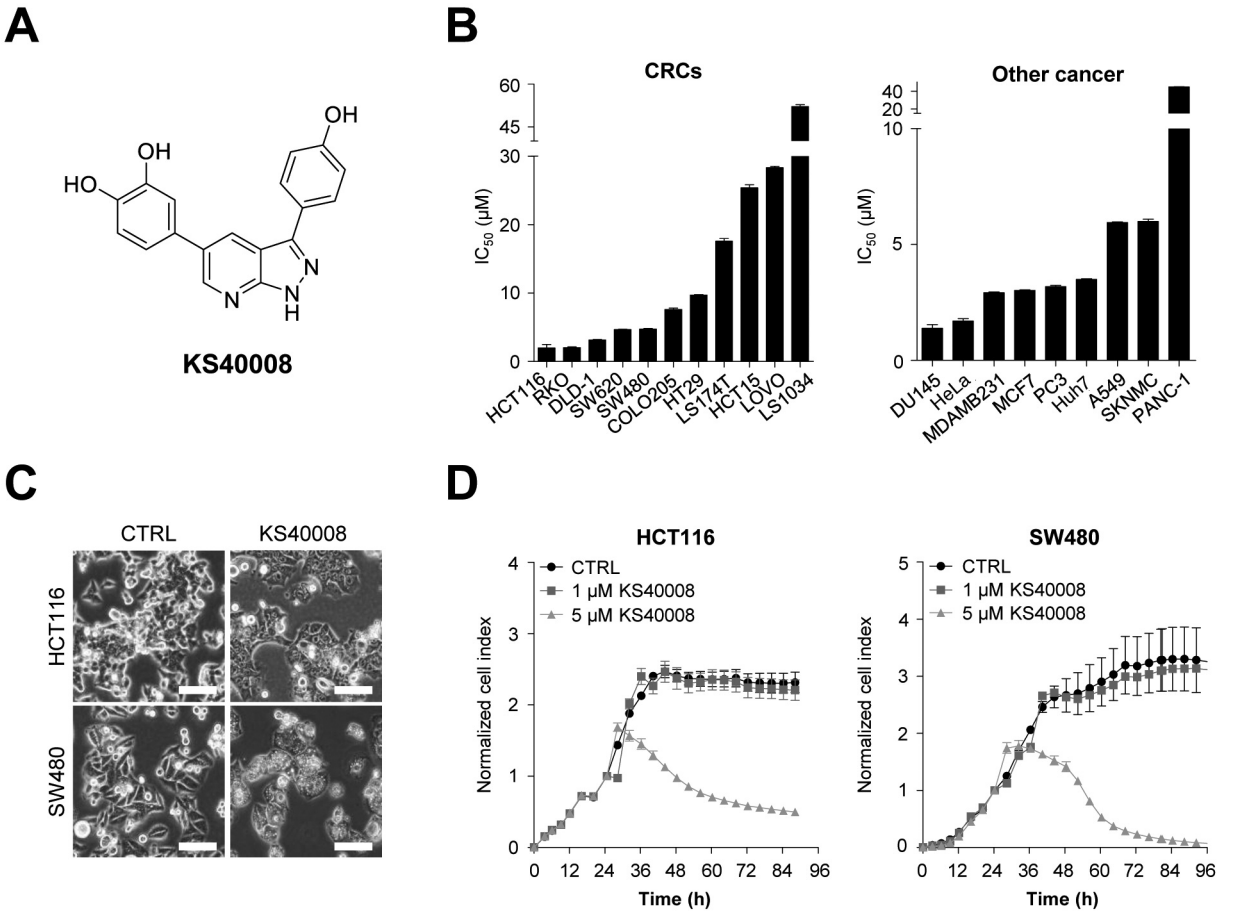

Figure 1. *KS40008 exhibited significant cytotoxicity in cancer cell lines. A: Structure of KS40008. B: Half-maximal inhibitory concentration (IC_{50}) values for KS40008 in colorectal cancer (CRC) and other cancer cell lines. C: Morphological changes in HCT116 and SW480 cells after 24 h of KS40008 treatment (5 μM). Representative images were taken under a microscope (original magnification, ×100). D: Real-time cell analysis screening of KS40008 in HCT116 and SW480 cell lines. Cells were plated at 0 h and KS40008 was administered at 24 h. Cell growth was then monitored until 96 h and the results are indicated as the mean±SEM (n=3).*

(4×10^4 cells per well) in a Seahorse XFe24 cell culture microplate. The plate was incubated for 24 h at 37˚C to allow the adhesion of the seeded cells. Growth medium was exchanged with Seahorse XF Base Medium (pH 7.4) supplemented with pyruvate, glutamine, and glucose at the same concentration as the supplemental composition of the growth medium. To investigate the altered metabolic potential of KS40008-treated cells, 1 μM oligomycin and 1 μM carbonyl cyanide-4 (trifluoromethoxy) phenylhydrazone were added to the injection ports of the sensor cartridges. To obtain the image-based normalization value, after the injection of Hoechst33342, fluorescence microscopic images were captured by Cytation 1 (BioTek Instruments, Winooski, VT, USA). The cell energy phenotype test (Agilent Technologies Inc.) was performed according to the manufacturer's instructions. The metrics for two major energy pathways in the cell, namely the oxygen consumption rate (OCR) and the extracellular acidification rate (ECAR), were calculated using the Seahorse XF Report Generator program after the measurement of basal metabolic flux values.

Reactive oxygen species (ROS) measurement. To detect cellular ROS levels, we utilized 2',7'-dichlorodihydrofluorescein diacetate (DCFDA) staining, a general indicator of ROS. Cells were plated at a density of 2×10^4 cells/ml in 96-well plates and then treated with 5 μM KS40008 for 24 h. DCFDA solution was added directly to the cells at a final working concentration of 1 μM and incubated for 10 min. Cells were then washed twice with phosphate-buffered saline and visualized with Operetta CLS (PerkinElmer) at excitation and emission wavelengths of 488 and 525 nm, respectively.

Quantitative real-time polymerase chain reaction (qRT-PCR). Total RNA was extracted using an RNA extraction kit (GeneAll, Seoul, Republic of Korea). The isolated RNA was reverse-transcribed to cDNA (Applied Biosystems Inc.). qRT-PCR was then conducted using SYBR Green Master Mix (Applied Biosystems Inc.) according to the manufacturer's instructions. The following primers were used: *DYRK1A*, forward: 5'-CTGGTCCAGGTCTGG TAGGT-3', reverse: 5'-ACTTTCAGAGATTGCTGATGCC-3'; *DYRK1B*, forward: 5'-TTGTGGTCGCCATTTTGCTG-3', reverse: 5'-AAGG

GGACTCAAACTGCTCG-3'; *DYRK2*, forward: 5'-ATTTCACCT TCCGCAACCAC-3', reverse: 5'-TCTCGGGCTTAAGGTCACAG-3'; *EIF2A,* forward: 5'-GCCAAATTGCCCTATCTCAA-3', reverse: 5'-CAGAAAAATGGGCAAAGGAA-3'; *ATF4,* forward: 5'-CTTCA CCTTCTTACAACCTCTTC-3', reverse: 5'-GTAGTCTGGCTTCCT ATCTCC-3'; *CHOP,* forward: 5'-CAGAACCAGCAGAGGTC ACA-3', reverse: 5'-AGCTGTGCCACTTTCCTTTC-3'; beclin 1 (*BECN1)*, forward: 5'-GAGCCATTTATTGAAACTCGCCA-3', reverse: 5'-CCTCCCCG ATCAGAGTGAA-3'; autophagy-related 4B cysteine peptidase (*ATG4B)*, forward: 5'-TATGATACTCTCC GGTTTGCTGA-3', reverse: 5'-GTTCCCCC AATAGCTGGAAAG-3'; and β-actin (*ACTB*) forward: 5'-TTGCC GACAGGATG CAGAAG-3', reverse: 5'-AGGTGGACAGCGAG GCCAGG-3'. Relative gene expression was quantitatively analyzed using the $2^{-\Delta\Delta Ct}$ method, and *ACTB* was used as an internal control for normalization.

Western blotting. To extract proteins, cells were lysed with radioimmunoprecipitation assay buffer containing phosphatase and protease inhibitors. Protein concentrations were quantitatively evaluated using the Bradford protein assay, with bovine serum albumin used as a standard. Equal amounts of proteins were separated using sodium dodecyl sulfate-polyacrylamide gel electrophoresis and immunoblotting using standard protocols. The following primary antibodies were used for immunoblotting: DYRK1B (2703S), phospho-EIF2A (Ser51) (9721S), EIF2A (9722S), ATF4 (11815S), CHOP (2895S), and microtubule-associated protein 1A/1B light chain 3B (LC3B) (2775S) antibodies were purchased from Cell Signaling Technology (Danvers, MA, USA). DYRK2 (sc-66867) and ACTB (sc-47778) antibodies were obtained from Santa Cruz Biotechnology, Inc. (Dallas, CA, USA). DYRK1A antibody (ab69811) was purchased from Abcam (Cambridge, UK).

Transmission electron microscopy. HCT116 cells were treated with KS40008 for 24 h. Cells were collected and fixed with 2% paraformaldehyde and 2% glutaraldehyde. Cells were then observed using transmission electron microscopy (JEOL; JEO-1011, Tokyo, Japan).

Fluorescence microscopy. HCT116 and SW480 cell lines cultured on 96-well plates were treated with 5 μM KS40008 for 24 h. Cells were washed twice with PBS and fixed for 15 min with 4% (w/v) paraformaldehyde. Cells were then permeabilized with 0.1% Triton X-100 in PBS for 10 min and blocked with 10% normal goat serum (Abcam). LC3B antibody (LifeSpan BioSciences, Inc., Seattle, WA, USA) was used as the primary antibody at 4˚C overnight. Cells were then incubated with 2 μg/ml Alexa Fluor 594 (Invitrogen, Carlsbad, CA, USA) for 2 h and washed three times with phosphate-buffered saline. To stain the nucleus, 1 μM of 4', 6-diamidino-2-phenylindole solution was added to each well for 10 min. Images were then taken on an Operetta CLS (PerkinElmer) and fluorescence intensity was quantitatively analyzed using four random fields using Harmony software.

To investigate the effect on mitochondria of KS40008, HCT116 and SW480 cells were treated with 5 μM KS40008 for 24 h and then stained with MitoTracker Deep Red FM (Invitrogen) to assess the mitochondrial area. Fluorescent microscopy images were recorded with an Operetta CLS (PerkinElmer).

Statistical analysis. All experiments were performed in triplicate, and the results are presented as the mean±standard error. Statistical analyses were performed using GraphPad Prism software and Student's *t*-test. Statistical significance was set at $p<0.05$.

Results

KS40008 showed potent cytotoxicity towards several cancer cell lines. After identifying a novel DYRK1A/B inhibitor, KS40008 (15), we investigated the molecular mechanisms of KS40008 and its cytotoxicity in diverse cancer cell lines. To determine the cytotoxic effect of KS40008 on different cancer cell lines, we measured cell viability using the CCK-8 assay. KS40008 exhibited remarkable growth-inhibitory effects on several cancer cell lines, with divergent IC_{50} values, ranging from 1.4-52.1 μM (Figure 1B). Among these cancer cell lines, HCT116 and SW480 cell lines particularly displayed dramatic morphological changes that resulted in an abundance of cytoplasmic autophagic vacuoles as well as expansion of cell size when observed under a microscope after 24 h of KS40008 treatment (Figure 1C).

To confirm the effects of KS40008 on proliferation, we examined the cell growth of HCT116 and SW480 cell lines using real-time cell analysis. Non-treated cells maintained aggressive proliferation, whereas cells treated with 5 μM KS40008 displayed growth suppression, reflected by a reduction in the CI value 24 h after administration (Figure 1D). Overall, these results demonstrated that KS40008, a novel DYRK1A/B inhibitor, exhibited superb cytotoxicity.

KS40008 triggered metabolic reprogramming in CRC cells. Since metabolic flux is essential for understanding cellular metabolism, oxidative phosphorylation and glycolysis were determined using OCR and ECAR, respectively. To investigate whether KS40008 affected metabolic reprogramming, we measured metabolic parameters using an XFe 24 Analyzer. The OCR and ECAR were intensely reduced in HCT116 and SW480 cell lines after treatment with 5 μM and 10 μM KS40008 (Figure 2A and B). Both cell lines exhibited a reduction in OCR level in both basal and spare respiratory capacity conditions (Figure 2C) after treatment with 5 μM and 10 μM KS40008. The ratio of OCR to ECAR was utilized as an indicator of the metabolic switch in the XF cell energy map. We found that KS40008-treated cells entered quiescence more readily compared to vehicle-treated cells as shown by the reduced OCR and ECAR levels (Figure 2D). In addition, using fluorescence microscopy, we observed disruption of mitochondrial structure by KS40008 treatment (Figure 2E). These results indicated that KS40008 stimulated the metabolic reprogramming of HCT116 and SW480 cell lines by reducing mitochondrial respiration.

KS40008-induced autophagy was dependent on mitochondrial stress and ER stress. Since the DYRK1A/B-inhibitory effect of KS40008 was demonstrated by an enzymatic assay (15),

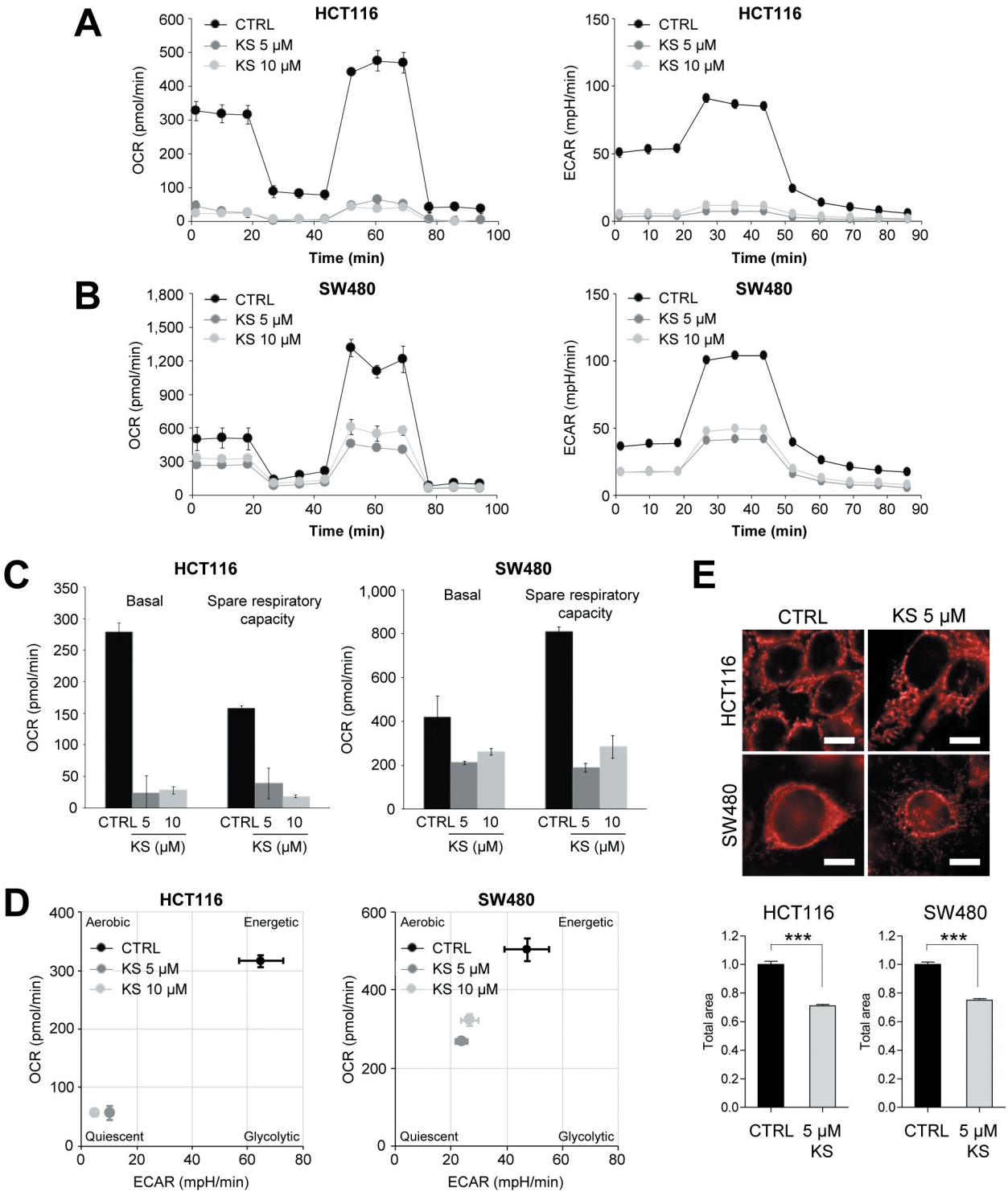

Figure 2. *KS40008 (KS) induced mitochondrial dysfunction through the reduction of oxidative phosphorylation and glycolysis, as assessed by oxygen consumption rate (OCR) and extracellular acidification rate (ECAR), respectively. The OCR and ECAR were measured in HCT116 (A) and SW480 (B) cell lines following 24-h treatment with 5 and 10 μM KS40008. C: OCR levels in basal HCT116 and SW480 cells and cells with spare respiratory capacity were assessed after treatment with KS40008 (5 and 10 μM) for 24 h using a Seahorse XFe24 Analyzer. D: XF cell energy map of KS40008 in HCT116 and SW480 cell lines. Normalized OCR and ECAR data were plotted to reveal the relative metabolic profiles. E: HCT116 and SW480 cells were treated with 5 μM KS40008 for 24 h and then stained with MitoTracker Deep Red FM. Total mitochondrial area was analyzed using four random fields using Harmony software. ***Significantly different at p<0.005.*

immunoblotting was employed to detect the changes in DYRK protein expression caused by KS40008. KS40008 generally reduced DYRK1A/B protein expression, whereas the level of DYRK2 remained constant in HCT116 and SW480 cell lines (Figure 3A). In addition, to examine whether KS40008 induced autophagy due to morphological changes, we measured the expression of LC3B protein, a key marker of autophagy. LC3B protein expression increased after 24 h of KS40008 treatment, suggesting that KS40008-mediated inhibition of DYRK1A/B enhanced autophagic cell death in CRC cell lines (Figure 3A). As autophagy is activated by ER stress, we wondered if the autophagic cell death caused by KS40008-induced DYRK1A/B inhibition was activated by ER stress. KS40008 remarkably activated the expression of ER stress-sensor proteins, phospho-EIF2A, ATF4, and CHOP in a dose-dependent manner (Figure 3A). The transcriptional activity of ER stress and autophagy genes was further quantified and revealed an increase in mRNA expression of *EIF2A, ATF4, CHOP, BECN1,* and *ATG4B* after KS40008 treatment, demonstrating the induction of ER stress-mediated autophagy in HCT116 and SW480 cell lines (Figure 3B), whereas KS40008 increased the transcription of DYRKs. Moreover, KS40008 activated the formation of autophagosomes, resulting in autophagic cell death, as observed using transmission electron microscopy (Figure 3C) and immunofluorescence images showed LC3B-positive autophagic vacuoles in CRC cells after treatment with KS40008 for 24 h (Figure 3D).

We then determined whether KS40008-induced ER stress was involved in ROS generation. As shown in Figure 3E, KS40008 significantly enhanced ROS production compared to the control cells. These results suggested that KS40008 stimulated ER stress and ROS through the suppression of DYRK1A/B-induced mitochondrial dysfunction, which ultimately led to autophagic cell death.

KS40008 displayed superior cytotoxicity to CRC organoids compared to 5-FU. In addition, we assessed the potential cytotoxicity of KS40008 using 13 established CRC organoids. To analyze the cytotoxic effect of KS40008 on CRC organoid models, 5-FU, which is a classic chemotherapeutic drug, was tested simultaneously. CRC organoids were treated with different concentrations (0-100 μM) of KS40008 and 5-FU for 5 days and monitored for conformational changes. Cell viability was evaluated using CellTiter-Glo. After 5 days of KS40008 treatment, collapse of conventional structures and formations of organoids were induced by KS40008, indicating a complete inhibition of proliferation, with divergent IC_{50} values ranging from 0.6 to 22.5 μM (Figure 4A and B). 5-FU-treated organoids showed similar morphological changes only at a 10-fold higher concentration than that of KS40008, with IC_{50} cytotoxicity ranging from 10.6 to 100 μM (Figure 4A and B). Taken together, these results revealed that KS40008 has potential to be used as a promising therapeutic agent against CRC.

Discussion

CRC is the second most aggressive cancer type, accounting for 9.2% of all cancer mortality (18) and is associated with lower response to standard therapy and acquired drug resistance. As few effective therapeutic agents exist in the treatment of CRC, novel therapeutic approaches are required to improve patient outcomes.

Members of the DYRK protein family are classified as either class I (DYRK1A and DYRK1B) or class II (DYRK2, DYRK3, and DYRK4) based on sequence homologies (19). The functional properties of DYRKs are highly correlated with the proliferation of cancer cells (20). In particular, DYRK1A and DYRK1B are able to induce cell-cycle exit, and their phosphorylation can drive S-phase entry through the induction of proteasome-dependent degradation of cyclin D1 and c-MYC (13, 21, 22). DYRK2 is also involved in cell-cycle regulation but is down-regulated in cancer, indicating an limited spectrum in the anticancer efficacy of the DYRK family (23). In addition, there are few studies on DYRK3 and DYRK4 (11, 24). Of note, DYRK1A/B is overexpressed in certain cancer types and is considered a potential oncogene (11). Therefore, DYRK1A/B is a promising target for novel chemotherapy against cancer.

KS40008, which has a 1*H*-pyrazolo[3,4-*b*]pyridine core, was identified as a novel DYRK1A/B inhibitor and exhibited superior enzymatic activity, with IC_{50} values ranging from 3 to 5 nM, as well as measurable cytotoxicity compared to numerous derivatives of this compound (15). In this study, we demonstrated that KS40008 inhibited DYRK1A/B in CRC cells, which stimulated autophagy through mitochondrial-dependent ER stress. In addition, we found that KS40008 activated the EIF2A–ATF4 pathway and, in turn, led to the induction of CHOP and ROS formation. However, a further detailed study on KS40008-induced ER stress and ROS formation should be conducted, as the mechanism of ROS generation by KS40008 remains unclear.

Mitochondria are the pivotal organelles for respiration, energy supply, and biosynthesis of metabolites in eukaryotic cells (25). The protein translocase of the outer membrane 70 (TOM70), which represents the main import receptor in mitochondria, is phosphorylated by DYRK1A/B, indicating that DYRK1A/B is important in regulating mitochondrial function (26-29). Inhibition of DYRK1A/B leads to the failure of $TOM70^{Ser91}$ phosphorylation, further causing the impairment of import of proteins involved in sustaining numerous biological functions (30). In our study, KS40008 suppressed oxidative phosphorylation and glycolysis, suggesting that mitochondrial metabolism can be reprogrammed through DYRK1A/B inhibition. Further study on KS40008-induced mitochondrial dysfunction is required. Disruption of mitochondrial metabolism by KS40008 was associated with ER stress-induced autophagic cell death (13, 31), highlighting the uncommon properties of KS40008 (Figure 5).

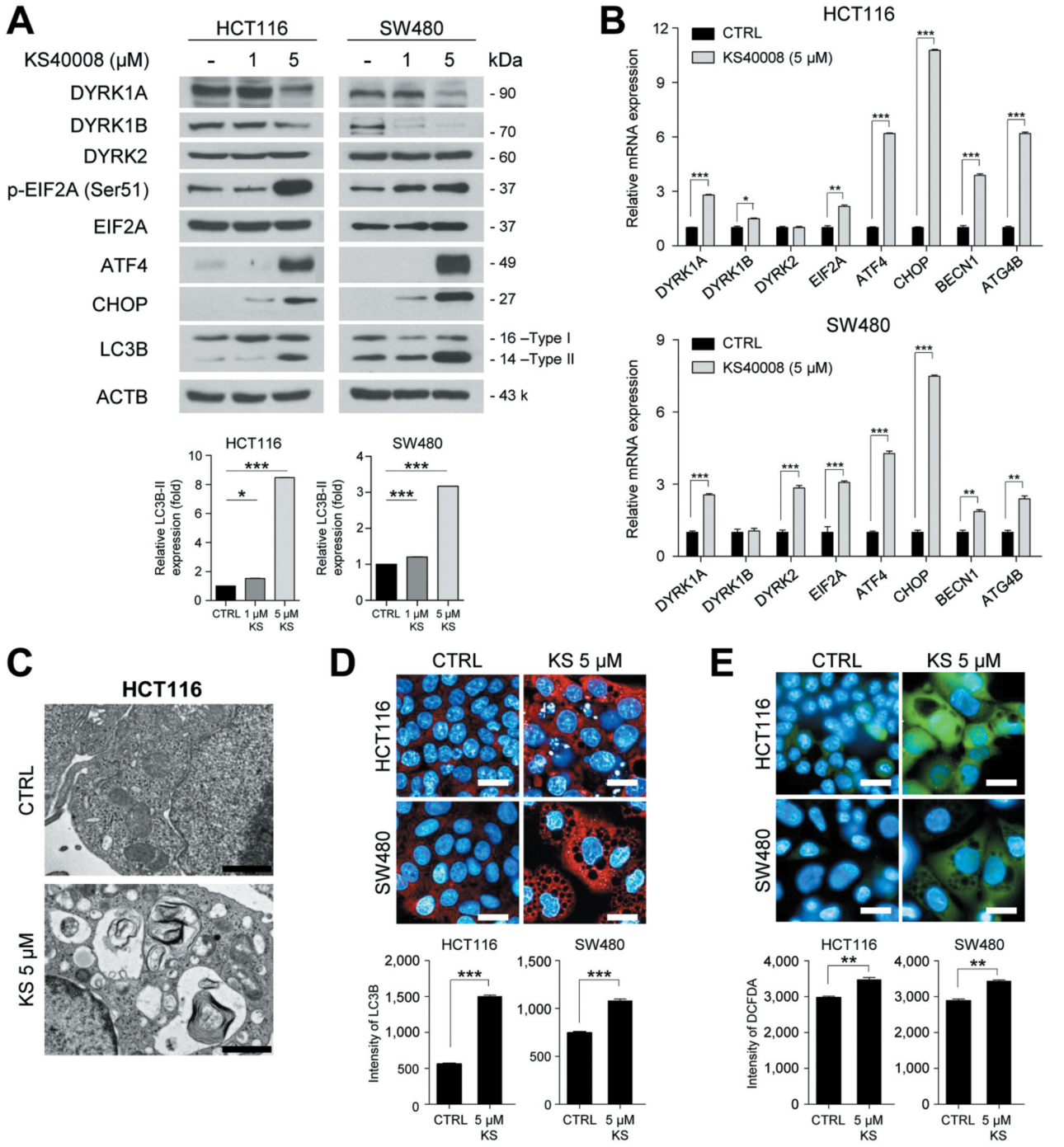

Figure 3. *KS40008 promoted autophagy through the induction of endoplasmic reticulum (ER) stress. A: Western blot analysis was used to detect the expression of dual-specificity tyrosine phosphorylation-regulated kinase family (DYRK1A, DYRK1B, and DYRK2), ER stress, and autophagy-related proteins phospho-eukaryotic translation initiation factor 2A (EIF2A), activating transcription factor 4 (ATF4), C/EBP homologous protein (CHOP) and microtubule-associated protein 1A/1B light chain 3B (LC3B) in HCT116 and SW480 cell lines after treatment with KS40008 (1 and 5 μM) for 24 h. The LC3B-II expression was quantified using image J software. B: Quantitative real-time polymerase chain reaction was used to assess the mRNA expression of autophagy-related genes (EIF2A, ATF4, CHOP, beclin1; BECN1, autophagy related 4B cysteine peptidase; ATG4B) in HCT116 and SW480 cells treated with KS40008 for 24 h. C: Representative transmission electron microscopy images in HCT116 cell treated with KS40008 (5 μM) for 24 h. Scale bars in figures are 1000 nm. D: Representative immunofluorescence images of LC3B (red) and 4',6-diamidino-2-phenylindole (DAPI) (blue) in HCT116 and SW480 cells treated with KS40008 (5 μM) for 24 h. The intensity of LC3B was analyzed using four random fields using Harmony software. E: Cellular reactive oxygen species (ROS) levels were measured using 2',7'-dichlorodihydrofluorescein diacetate (DCFDA) (green). Significantly different at: **p<0.001, *p<0.05 and ***p<0.005.*

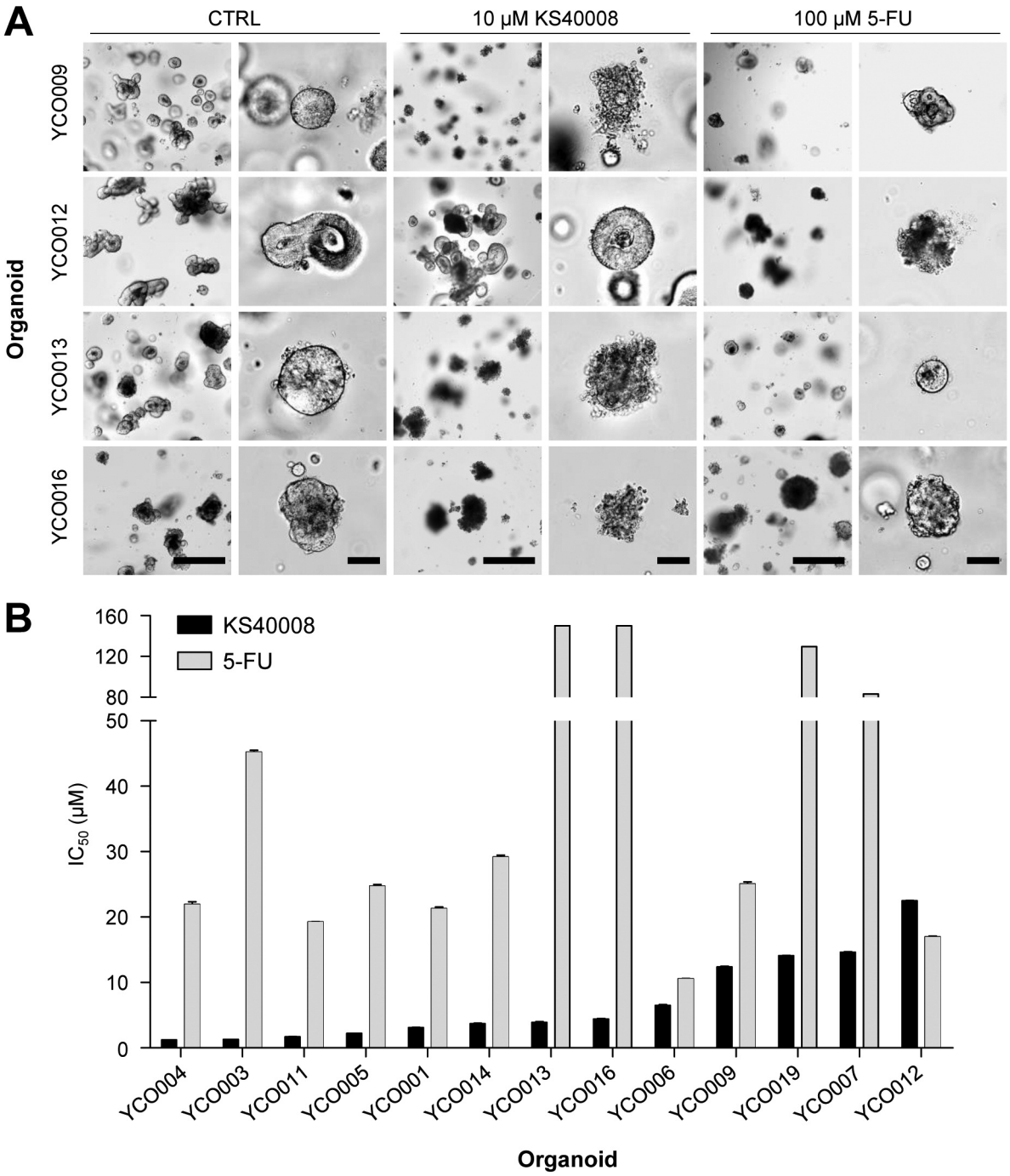

Figure 4. *KS40008 inhibited proliferation of colorectal cancer organoids. A: Representative bright-field images of KS40008 (10 μM) and 5-fluorouracil (5-FU) (100 μM) treated CRC organoids. Scale bar: 500 μm and 100 μm for images in left and right panels, respectively. B: Differential sensitivity of colorectal cancer organoids to KS40008 and 5-FU. The half maximal inhibitory concentration (IC_{50}) values were calculated using GraphPad Prism.*

In conclusion, we demonstrated the cell death mechanisms of KS40008, a novel DYRK1A/B inhibitor, in CRC cells. KS40008 was shown to affect the relationship between DYRK1A/B signaling and mitochondria-dependent ER stress-induced autophagy. Our results suggest that inhibition of DYRK1A/B by KS40008 has potential as a new form of effective therapeutic agent that might use synergistically with other drugs to strengthen antitumor activity (32). Further

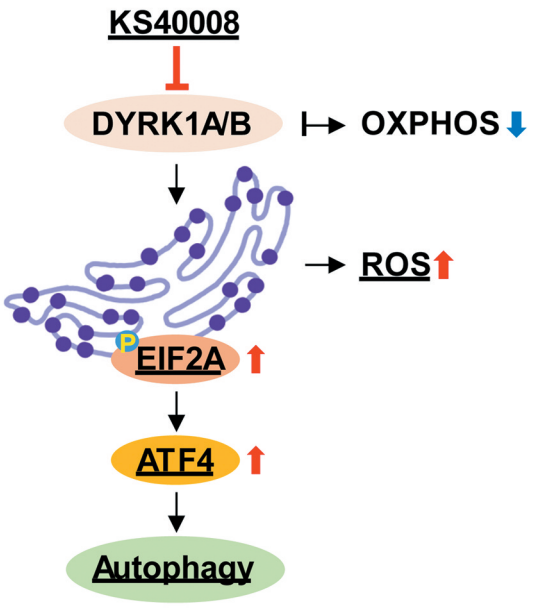

Figure 5. *KS40008 led to metabolic reprogramming through the inhibition of dual-specificity tyrosine phosphorylation-regulated kinase family (DYRK) 1A/B, prompting autophagy. Suppression of DYRK1A/B by KS40008 reduced oxidative phosphorylation (OXPHOS) reactions while triggering both endoplasmic reticulum (ER) stress and reactive oxygen species (ROS) generation. KS40008 up-regulated the eukaryotic translation initiation factor 2A (EIF2A)–activating transcription factor 4 (ATF4) signaling pathway and, subsequently, autophagic cell death in response to ER stress in colorectal cancer cells.*

studies should be performed to explore KS40008-induced autophagy pathways.

Conflicts of Interest

No conflicts of interest relevant to this article were reported.

Authors' Contributions

Conceived and designed the analysis: HL and SJS. Collected the data: JH, AP, HL, and SJS. Performed the analysis: JH, AP, DY, MK, JY, KYK, TIK, KSJ, HB, HL, and SJS. Wrote the article: JH, CK, HL, and SJS.

References

1 Wek RC, Jiang HY and Anthony TG: Coping with stress: eIF2 kinases and translational control. Biochem Soc Trans *34(Pt 1)*: 7-11, 2006. PMID: 16246168. DOI: 10.1042/BST20060007

2 Rozpedek W, Nowak A, Pytel D, Diehl JA and Majsterek I: Molecular basis of human diseases and targeted therapy based on small-molecule inhibitors of ER stress-induced signaling pathways. Curr Mol Med *17(2)*: 118-132, 2017. PMID: 28266275. DOI: 10.2174/1566524017666170306122643

3 Stutzmann GE and Mattson MP: Endoplasmic reticulum Ca(2+) handling in excitable cells in health and disease. Pharmacol Rev *63(3)*: 700-727, 2011. PMID: 21737534. DOI: 10.1124/pr.110.003814

4 Zhou S, Zhao L, Kuang M, Zhang B, Liang Z, Yi T, Wei Y and Zhao X: Autophagy in tumorigenesis and cancer therapy: Dr. Jekyll or Mr. Hyde? Cancer Lett *323(2)*: 115-127, 2012. PMID: 22542808. DOI: 10.1016/j.canlet.2012.02.017

5 White E: Deconvoluting the context-dependent role for autophagy in cancer. Nat Rev Cancer *12(6)*: 401-410, 2012. PMID: 22534666. DOI: 10.1038/nrc3262

6 White E and DiPaola RS: The double-edged sword of autophagy modulation in cancer. Clin Cancer Res *15(17)*: 5308-5316, 2009. PMID: 19706824. DOI: 10.1158/1078-0432.CCR-07-5023

7 Jia S, Xu X, Zhou S, Chen Y, Ding G and Cao L: Fisetin induces autophagy in pancreatic cancer cells via endoplasmic reticulum stress- and mitochondrial stress-dependent pathways. Cell Death Dis *10(2)*: 142, 2019. PMID: 30760707. DOI: 10.1038/s41419-019-1366-y

8 Tanabe M, Izumi H, Ise T, Higuchi S, Yamori T, Yasumoto K and Kohno K: Activating transcription factor 4 increases the cisplatin resistance of human cancer cell lines. Cancer Res *63(24)*: 8592-8595, 2003. PMID: 14695168.

9 Igarashi T, Izumi H, Uchiumi T, Nishio K, Arao T, Tanabe M, Uramoto H, Sugio K, Yasumoto K, Sasaguri Y, Wang KY, Otsuji Y and Kohno K: Clock and ATF4 transcription system regulates drug resistance in human cancer cell lines. Oncogene *26(33)*: 4749-4760, 2007. PMID: 17297441. DOI: 10.1038/sj.onc.1210289

10 Jayasooriya RGPT, Dilshara MG, Karunarathne WAHM, Molagoda IMN, Choi YH and Kim GY: Camptothecin enhances c-Myc-mediated endoplasmic reticulum stress and leads to autophagy by activating Ca^{2+}-mediated AMPK. Food Chem Toxicol *121*: 648-656, 2018. PMID: 30266318. DOI: 10.1016/j.fct.2018.09.057

11 Soppa U and Becker W: DYRK protein kinases. Curr Biol *25(12)*: R488-R489, 2015. PMID: 26079075. DOI: 10.1016/j.cub.2015.02.067

12 Chen Y, Wang S, He Z, Sun F, Huang Y, Ni Q, Wang H, Wang Y and Cheng C: Dyrk1B overexpression is associated with breast cancer growth and a poor prognosis. Hum Pathol *66*: 48-58, 2017. PMID: 28554575. DOI: 10.1016/j.humpath.2017.02.033

13 Becker W: Emerging role of DYRK family protein kinases as regulators of protein stability in cell cycle control. Cell Cycle *11(18)*: 3389-3394, 2012. PMID: 22918246. DOI: 10.4161/cc.21404

14 Radhakrishnan A, Nanjappa V, Raja R, Sathe G, Puttamallesh VN, Jain AP, Pinto SM, Balaji SA, Chavan S, Sahasrabuddhe NA, Mathur PP, Kumar MM, Prasad TS, Santosh V, Sukumar G, Califano JA, Rangarajan A, Sidransky D, Pandey A, Gowda H and Chatterjee A: A dual specificity kinase, DYRK1A, as a potential therapeutic target for head and neck squamous cell carcinoma. Sci Rep *6*: 36132, 2016. PMID: 27796319. DOI: 10.1038/srep36132

15 Park A, Hwang J, Lee JY, Heo EJ, Na YJ, Kang S, Jeong KS, Kim KY, Shin SJ and Lee H: Synthesis of novel 1H-Pyrazolo[3,4-b]pyridine derivatives as DYRK 1A/1B inhibitors. Bioorg Med Chem Lett *47*: 128226, 2021. PMID: 34182093. DOI: 10.1016/j.bmcl.2021.128226

16 Ku M, Kang M, Suh JS and Yang J: Effects for sequential treatment of siAkt and paclitaxel on gastric cancer cell lines. Int J Med Sci *13(9)*: 708-716, 2016. PMID: 27648001. DOI: 10.7150/ijms.15501

17 Limame R, Wouters A, Pauwels B, Fransen E, Peeters M, Lardon F, De Wever O and Pauwels P: Comparative analysis of dynamic cell viability, migration and invasion assessments by novel real-time technology and classic endpoint assays. PLoS One *7(10)*: e46536, 2012. PMID: 23094027. DOI: 10.1371/journal.pone.0046536

18 Bray F, Ferlay J, Soerjomataram I, Siegel RL, Torre LA and Jemal A: Global cancer statistics 2018: GLOBOCAN estimates of incidence and mortality worldwide for 36 cancers in 185 countries. CA Cancer J Clin *68(6)*: 394-424, 2018. PMID: 30207593. DOI: 10.3322/caac.21492

19 Aranda S, Laguna A and de la Luna S: DYRK family of protein kinases: evolutionary relationships, biochemical properties, and functional roles. FASEB J *25(2)*: 449-462, 2011. PMID: 21048044. DOI: 10.1096/fj.10-165837

20 Gao J, Zhao Y, Lv Y, Chen Y, Wei B, Tian J, Yang Z, Kong F, Pang J, Liu J and Shi H: Mirk/Dyrk1B mediates G0/G1 to S phase cell cycle progression and cell survival involving MAPK/ERK signaling in human cancer cells. Cancer Cell Int *13(1)*: 2, 2013. PMID: 23311607. DOI: 10.1186/1475-2867-13-2

21 Vilenchik M, Kuznetsova A, Frid M, Duey M, Damiani A, De leon L, Law J, Golbin D, Shishkina L and Potapova O: Implication of DYRK1B kinase in dormant glioblastoma cancers and utilization of DYRK1B inhibitors as a novel therapeutic strategy for glioblastoma. Journal of Clinical Oncology *37(15_suppl)*: e14670-e14670, 2020. DOI: 10.1200/JCO.2019.37.15_suppl.e14670

22 Ashford AL, Dunkley TP, Cockerill M, Rowlinson RA, Baak LM, Gallo R, Balmanno K, Goodwin LM, Ward RA, Lochhead PA, Guichard S, Hudson K and Cook SJ: Identification of DYRK1B as a substrate of ERK1/2 and characterisation of the kinase activity of DYRK1B mutants from cancer and metabolic syndrome. Cell Mol Life Sci *73(4)*: 883-900, 2016. PMID: 26346493. DOI: 10.1007/s00018-015-2032-x

23 Li L, Wei JR, Song Y, Fang S, Du Y, Li Z, Zeng TT, Zhu YH, Li Y and Guan XY: TROAP switches DYRK1 activity to drive hepatocellular carcinoma progression. Cell Death Dis *12(1)*: 125, 2021. PMID: 33500384. DOI: 10.1038/s41419-021-03422-3

24 Taira N, Mimoto R, Kurata M, Yamaguchi T, Kitagawa M, Miki Y and Yoshida K: DYRK2 priming phosphorylation of c-Jun and c-Myc modulates cell cycle progression in human cancer cells. J Clin Invest *122(3)*: 859-872, 2012. PMID: 22307329. DOI: 10.1172/JCI60818

25 Nunnari J and Suomalainen A: Mitochondria: in sickness and in health. Cell *148(6)*: 1145-1159, 2012. PMID: 22424226. DOI: 10.1016/j.cell.2012.02.035

26 Brix J, Dietmeier K and Pfanner N: Differential recognition of preproteins by the purified cytosolic domains of the mitochondrial import receptors Tom20, Tom22, and Tom70. J Biol Chem *272(33)*: 20730-20735, 1997. PMID: 9252394. DOI: 10.1074/jbc.272.33.20730

27 MacPherson L and Tokatlidis K: Protein trafficking in the mitochondrial intermembrane space: mechanisms and links to human disease. Biochem J *474(15)*: 2533-2545, 2017. PMID: 28701417. DOI: 10.1042/BCJ20160627

28 Palmieri F: Diseases caused by defects of mitochondrial carriers: a review. Biochim Biophys Acta *1777(7-8)*: 564-578, 2008. PMID: 18406340. DOI: 10.1016/j.bbabio.2008.03.008

29 Wiedemann N, Pfanner N and Ryan MT: The three modules of ADP/ATP carrier cooperate in receptor recruitment and translocation into mitochondria. EMBO J *20(5)*: 951-960, 2001. PMID: 11230119. DOI: 10.1093/emboj/20.5.951

30 Walter C, Marada A, Suhm T, Ernsberger R, Muders V, Kücükköse C, Sánchez-Martín P, Hu Z, Aich A, Loroch S, Solari FA, Poveda-Huertes D, Schwierzok A, Pommerening H, Matic S, Brix J, Sickmann A, Kraft C, Dengjel J, Dennerlein S, Brummer T, Vögtle FN and Meisinger C: Global kinome profiling reveals DYRK1A as critical activator of the human mitochondrial import machinery. Nat Commun *12(1)*: 4284, 2021. PMID: 34257281. DOI: 10.1038/s41467-021-24426-9

31 Kimmelman AC and White E: Autophagy and tumor metabolism. Cell Metab *25(5)*: 1037-1043, 2017. PMID: 28467923. DOI: 10.1016/j.cmet.2017.04.004

32 Li YL, Ding K, Hu X, Wu LW, Zhou DM, Rao MJ, Lin NM and Zhang C: DYRK1A inhibition suppresses STAT3/EGFR/Met signalling and sensitizes EGFR wild-type NSCLC cells to AZD9291. J Cell Mol Med *23(11)*: 7427-7437, 2019. PMID: 31454149. DOI: 10.1111/jcmm.14609

Received October 1, 2021
Revised November 9, 2021
Accepted November 12, 2021